Journal of Ceramic Processing Research. Vol. 21, Special. 1, pp. s16~s22 (2020)
(Received 17 December 2019, Received in revised form 22 March 2020, Accepted 24 March 2020)
https://doi.org/10.36410/jcpr.2020.21.S1.s16

J O U R N A L O F
Ceramic Processing Research

Mechanical properties and electrical resistivity of SiC-TiC composites with nitrate sintering additives

Sung Min So[a,b], Hee Woong Hwang[a,c], Sam Heang Yi[a,c], Joo Seok Park[a,*], Kyoung Hun Kim[a], Kwang Ho Lee[d], Jongee Park[e] and Sung Gap Lee[c]

[a]*Korea Institute of Ceramic Engineering and Technology, Jinju, Korea*
[b]*Information Materials Lab. Materials Engineering, Inha University, Incheon, Korea*
[c]*Ceramic Engineering Department, Gyougsang National University, Jinju, Korea*
[d]*Booil Technology co., Ltd., Gunpo, Korea*
[e]*Department of Metallurgical and Materials Engineering, ATILIM University, Ankara, Turkey*

We fabricated SiC-TiC composites by hot-press sintering with aluminum and yttrium nitrate additive and evaluated crystal phase, relative density, microstructure, electrical resistivity and mechanical properties of the sintered body. And the effect of nitrate additive on the densification of SiC-TiC composites was compared with that of Al_2O_3 and Y_2O_3 additives. Because nitrate additives were uniformly dispersed in SiC and TiC mixture, it inhibited the growth of crystal grain between each other and formed fine and uniform microstructure, thereby improving mechanical properties and electrical resistivity. The electrical resistivity and flexural strength of the SiC-TiC composite with aluminum and yttrium nitrate additive were 2.3 Ω·cm and 652.3 MPa respectively.

Keywords: SiC-TiC, Composites, Mechanical properties, Electrical resistivity, Nitrate additive.

Introduction

Silicon carbide (SiC) forms tetrahedron basic structure by sp^3 hybrid orbital function of carbon (C) and silicon (Si), and strong covalent non-oxide having σ-bond between C and Si. It is a ceramic material with excellent mechanical properties such as hardness, strength, elastic modulus, and abrasion resistance compared to other ceramic materials and additionally has high thermal conductivity and stable properties to various acids and bases [1-5]. As a result, it is applied as a core component in various industries such as abrasives, heating elements, high temperature structural materials, heat exchangers, mechanical seals, bulletproof materials, and semiconductor manufacturing process parts [6-9]. SiC can be classified into β-SiC of cubic structure and α-SiC of a hexagonal and rhombohedral structure according to the crystal structure. The α-SiC has different polytypes according to the stacking sequences such as 4H, 6H, 15R, etc., and it is known that various physical and electrical properties are expressed by this crystal structure [10]. High purity SiC has a low electrical conductivity close to the insulator, but recently, there has been a growing interest in the application of SiC materials to the devices used in extreme environments such as high temperature, high power, and high frequency by controlling electric conductivity or an electrodischarge machining for the processing of semiconductor process equipment parts or complex shaped parts that require various electrical conductivity [11-13].

The electrical resistance of SiC can be lowered by doping nitrogen (N) atoms in the SiC lattice, sintering with liquid phase additives such as Al_2O_3, Y_2O_3, Sc_2O_3, etc. in nitrogen atmosphere, or adding conductive additives such as TiN, ZrN, TiC, TiB_2 which helps to improve electrical conductivity [14-16]. Among them, TiC has the highest hardness, modulus of elasticity, coefficient of thermal expansion, and lower electrical resistance than SiC. Therefore, when forming a composite with SiC it is expected to lower the electrical resistance and to improve mechanical properties compared to SiC monoliths through particle strengthening effect [17]. SiC-TiC composites can be prepared through liquid phase sintering with the addition of oxide sintering aids such as Y_2O_3, Al_2O_3-Y_2O_3, or reaction sintering through a reduction of TiO_2 added in SiC [18, 19]. In addition, pressure sintering methods such as hot press sintering and spark plasma sintering are used to manufacture products that are dense and have excellent mechanical properties [20].

The study of SiC-TiC composites has been mainly focused on improving mechanical properties such as fracture toughness through particle strengthening mechanism. It is known that residual stress due to

*Corresponding author:
Tel : +82-55-792-2775
Fax: +82-55-792-2796
E-mail: pjuju@kicet.re.kr

mismatch of thermal expansion coefficient of TiC ($\alpha = 7.4 \times 10^{-6}\ K^{-1}$) particles uniformly dispersed in the SiC matrix ($\alpha = 4.5 \times 10^{-6}\ K^{-1}$) suppress the progress of cracks, thereby increasing the fracture toughness and strength. Furthermore, Wei and Becher reported that the fracture toughness increased by 50% when the TiC content in the SiC-TiC composite was 24.6 vol% [21-24]. On the other hand, researches on the electrical properties of SiC-TiC composites are rare. M. Khodaei et al. prepared a SiC-TiC composite showing an electrical resistance of $2.2 \times 10^5\ \Omega$·m by the reaction between TiO_2 and SiC [25].

Therefore, this study aims to manufacture low-resistance SiC-TiC composites with excellent mechanical properties using $Y_3Al_5O_{12}$ (yttrium aluminum garnet, YAG) as a liquid sintering aid. The electrical resistance of SiC-TiC composites is greatly influenced by the grain size of the components constituting the matrix, the amounts of additives, and the uniform dispersion [26]. Therefore, aluminum nitrate nonahydrate ($Al(NO_3)_3 \cdot 9H_2O$) and yttrium nitrate hexahydrate $Y(NO_3)_3 \cdot 6H_2O$ dissolved in ethanol are used as sintering aids to uniformly control the microstructure, and accordingly, the electrical resistance and mechanical properties were investigated.

Experimental

α-SiC powder (0.5 μm, 15C, Saint-Gobain, Norway) and TiC powder (2-3 μm, Pacific Particulate Materials, Canada) with 6H crystal structure were used as starting materials to prepare SiC-TiC composites. $Al(NO_3)_3 \cdot 9H_2O$ (98%, Sigma-Aldrich, USA) and $Y(NO_3)_3 \cdot 6H_2O$ (99.8%, Sigma-Aldrich, USA) were used as sintering aids. Here, Al_2O_3 (0.2 μm Sumitomo Chemical, Japan) and Y_2O_3 (2 μm, high Purity Chemical, Japan) were used as oxide sintering aids for comparison with nitrate sintering aids. The raw materials were weighted as shown in Table 1 and mixed mechanically for 12 h with SiC balls in a polypropylene jar using ethanol medium. The mixed slurry was dried and passed through 200 mesh sieve to prepare a SiC-TiC mixed powder. The prepared powder was placed in a graphite mold of 50 × 50 mm, and then sintered at 1,800-1,950 ºC for 1 h under 40 MPa pressure in a nitrogen atmosphere using a hot-press sintering furnace (SHP-30; Samyang Ceratech, South Korea) to form a SiC-TiC composite.

The density of the prepared SiC-TiC composites was measured using the Archimedes method, and the crystal phase analysis was performed using an X-ray diffractometer (Smart Lab, Rigaku, Japan). The SiC-TiC sintered body was tailored by 3×4×35 mm, and then the bending strength was measured by 3 point method under span 30 mm and head speed 0.5 mm/s according to ISO 14704 standard. Fracture toughness was calculated by measuring the indented crack length using the formula ($K_{IC} = 0.018\ (E/H)^{0.5}(P/C^{1.5})$) proposed by Miyoshi et al. [27]. E is the modulus of elasticity, H is the Vickers hardness, P is the indentation load, and C is half the average crack length. The microstructure of the sintered body was observed using FE-SEM (JSM-7100F; Jeol, Japan), and thermal conductivity was calculated by the equation (($k = \rho \cdot Cp \cdot D$ (k: thermal conductivity, ρ: density, Cp: heat capacity, D: thermal diffusion coefficient)) after measuring the thermal diffusion coefficient using a laser flash device (LFA 427, NETZSCH, Germany). The specific resistance of the SiC-TiC composites was measured using a resistance measuring instrument (CMT-SR1000N, Advanced Instrument Technology, USA).

Results and Discussion

Fig. 1 is a graph showing the relative density of the composite according to the sintering temperature. The relative density increased with increasing sintering temperature. Reaching a maximum value at 1,950 ºC. ST (SiC-30 vol% TiC) composition without sintering aid shows a low relative density of about 82.5-97.3% depending on the sintering temperature. However, STY (SiC-30 vol% TiC-2 vol% YAG) and STYN (SiC-30 vol% TiC-2 vol% YAG) compositions with the sintering

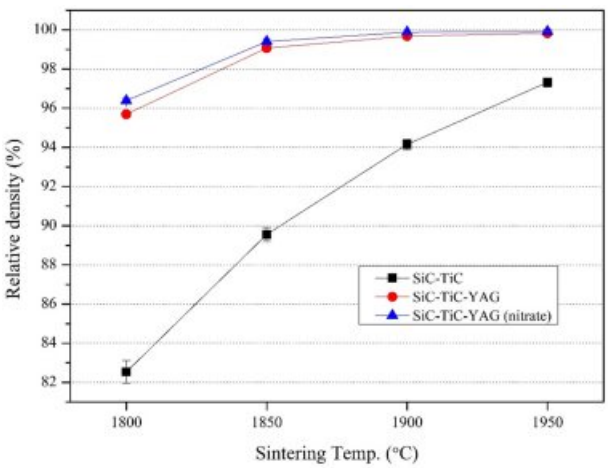

Fig. 1. Variation of relative density of SiC-TiC composites with the sintering temperature.

Table 1. Batch composition of SiC-TiC composite.

Sample	Batch composition (wt%)
ST [SiC-30 vol% TiC]	39.69 % α-SiC + 60.31 % TiC
STY [SiC-30 vol% TiC -2 vol% YAG]	39.21 % α-SiC + 57.87 % TiC + 1.25 % Al_2O_3 + 1.67 % Y_2O_3
STYN [SiC-30 vol% TiC -2 vol% YAG (nitrate)]	35.03 % α-SiC + 51.70 % TiC + 8.23 % $Al(NO_3)_3 \cdot 6H_2O$ + 5.04 % $Y(NO_3)_3 \cdot 9H_2O$

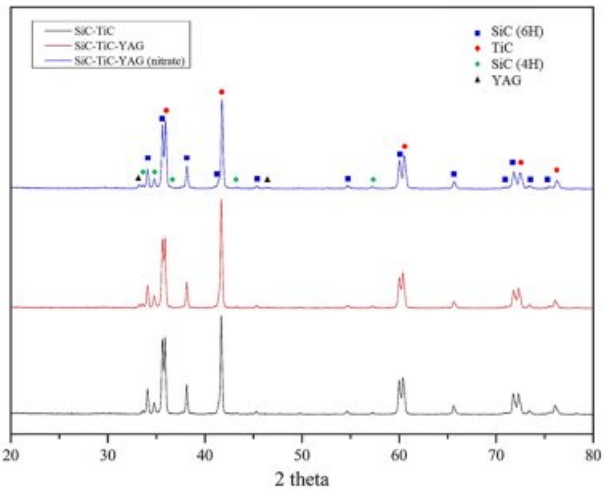

Fig. 2. XRD patterns of SiC-TiC sintered specimens at 1,950?**.**

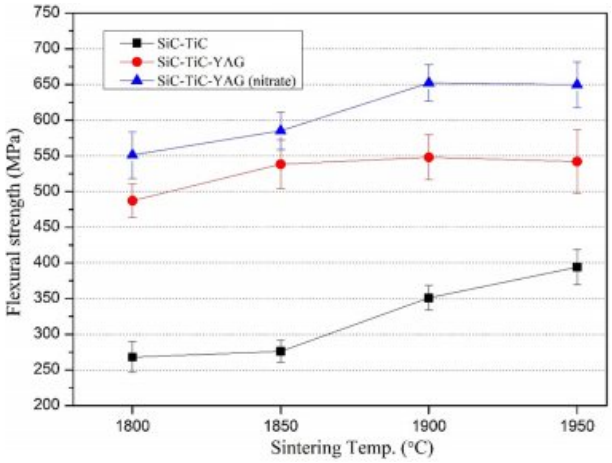

Fig. 3. Variation of flexural strength of SiC-TiC composites with the sintering temperature.

aid show the relative density of 99% or more at the sintering temperature of 1,850 ºC or higher. Comparing the relative densities of nitrate and oxide sintering aids, the relative density of STYN was slightly higher than that of STY from the sintering temperature of 1,800 °C and the relative density of STY was about 99.1% at 1,850 ºC while that of STYN was 99.4%. Through this result, it was found that nitrate sintering aid acts at a lower temperature than oxide sintering aid, promotes sintering, and helps to manufacture a denser sintered body [26].

Fig. 2 is the result of crystal phase analysis obtained through x-ray diffraction analysis. In all specimens, the main crystalline phases were analyzed by 6H-SiC and TiC, and 4H crystalline phases not included in the starting material were observed, indicating that SiC was phase-shifted from 6H to the 4H structure. This phase transition is thought to be caused by TiC because it occurs even in the composition without the sintering aid. In the compositions to which the sintering aid was added, the YAG crystal phase was observed from 1,800 °C, and it was confirmed that the liquid phase was formed at a low temperature and involved in densification.

The bending strength results of SiC-TiC composites were shown in Fig. 3. As the sintering temperature increases, the bending strength tends to increase, and when the sintering aid is not added, the relative density is low and the porosity is high, resulting in low strength. However, the composition with the sintering aid showed a high bending strength due to the increase of the relative density induced by rapid densification and showed a maximum value at 1,900 ºC. Therefore, it can be seen that the bending strength of STYN composition is better because the bending strength of STY is 547.9 MPa while the bending strength of STYN is 652.3 MPa. Also, as the sintering temperature increased from 1,900 ºC to 1,950 ºC, the bending strength decreased slightly. This is thought to be due to the grain growth at 1,950 ºC sintering temperature, as can be seen from Fig. 3 and 4. The reason why the bending strength is relatively high in the case of using the sintering aid of nitrate is thought to be that the fracture behavior is different as well as the influence of the high relative density. As seen in Fig. 3 and 4 of fractured surface FE-SEM images, the fracture shape of STY specimens shows more intragranular intergranular while that of STYN specimens shows both intragranular and intergranular. As such, the intergranular fracture in SiC-TiC composites is due to the strong interfacial bonds between the grains, and both the strength and fracture toughness are enhanced because more energy is consumed when cracks propagated through the grains of the composites. The addition of nitrate sintering aids showed that the YAG crystal size is smaller and more uniformly distributed in the microstructure than the oxide sintering aids, and as a result, strong interfacial bonds are formed between grains of the composite [28, 29].

Fig. 6 shows the Vickers hardness results of SiC-TiC composites according to the sintering temperature. The hardness tends to increase with increasing the sintering temperature, which is due to the increase in the sintering density and similar to the relative density graph (Fig. 1). At 1,900 ºC, the hardness of STY composition was 22.55 GPa and STYN composition was 52.14 GPa, which showed better hardness when nitrate sintering aid was added. The hardness decreases as the sintering temperature increases to 1,950 ºC, which may be due to grain growth as can be seen in the microstructure photographs (Fig. 4 and 5). The fracture toughness of composites with sintering temperature is shown in Fig. 7. Higher fracture toughness results in STYN composition with a nitrate sintering aid. Fracture toughness in grain-reinforced ceramic composites is known to be enhanced by residual stresses in thermal

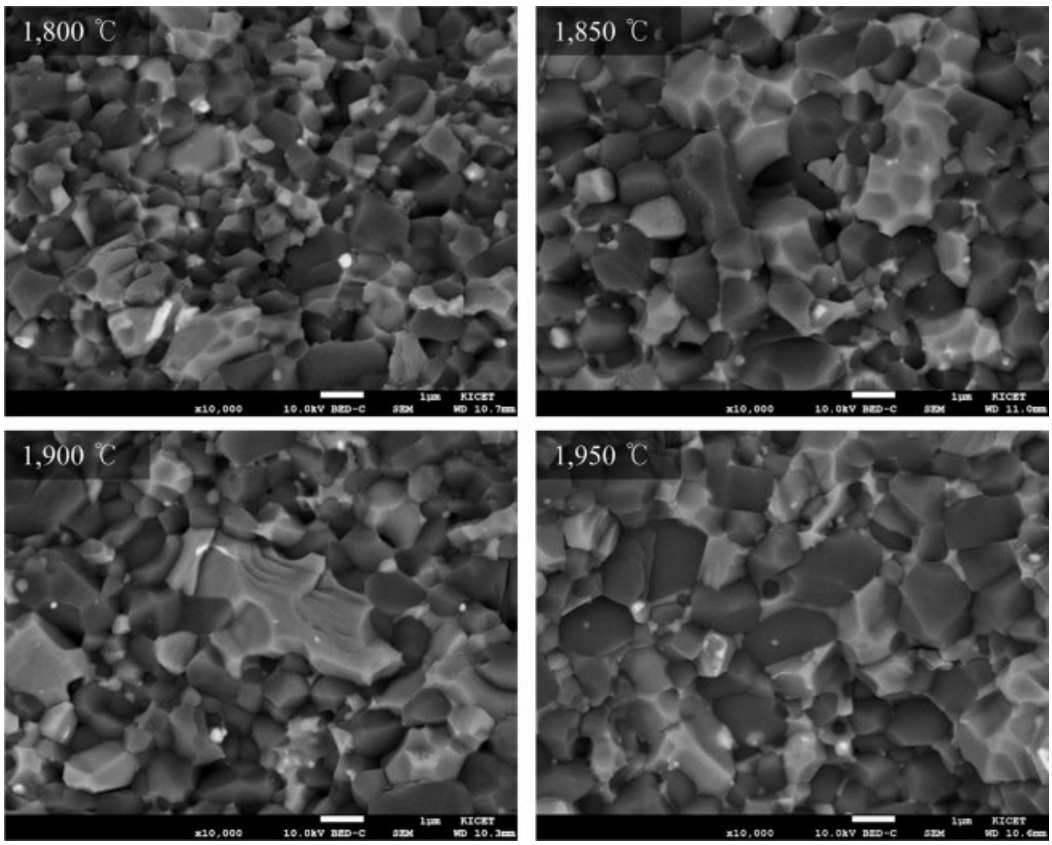

Fig. 4. Fracture surfaces of SiC-TiC-YAG composite.

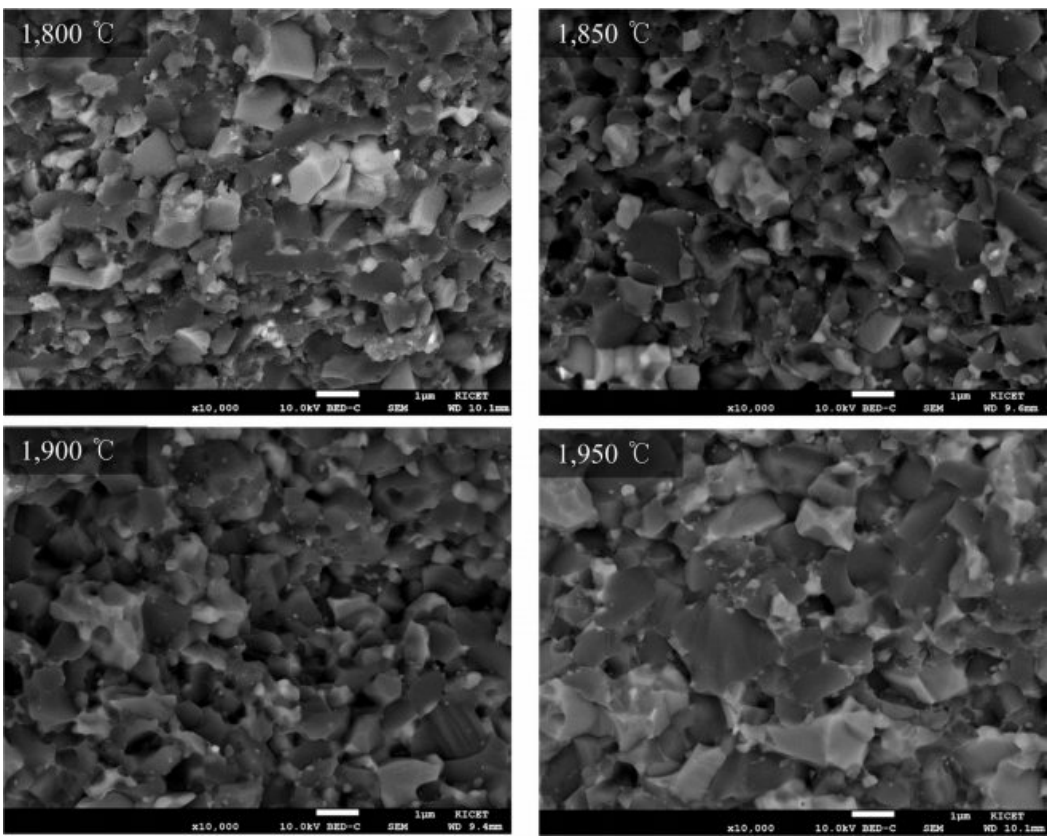

Fig. 5. Fracture surfaces of SiC-TiC-YAG (nitrate) composite.

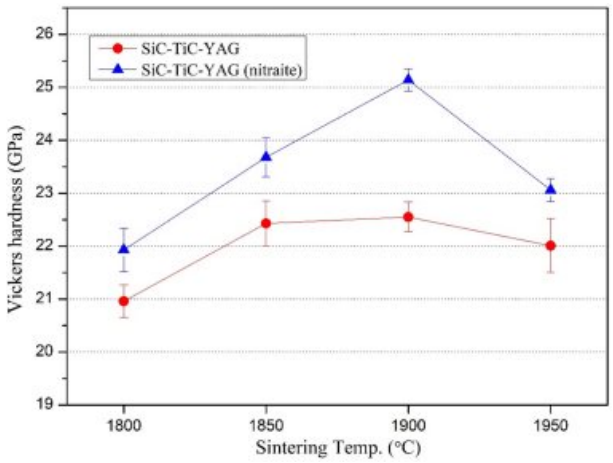

Fig. 6. Variation of Vickers hardness of SiC-TiC composites with the sintering temperature.

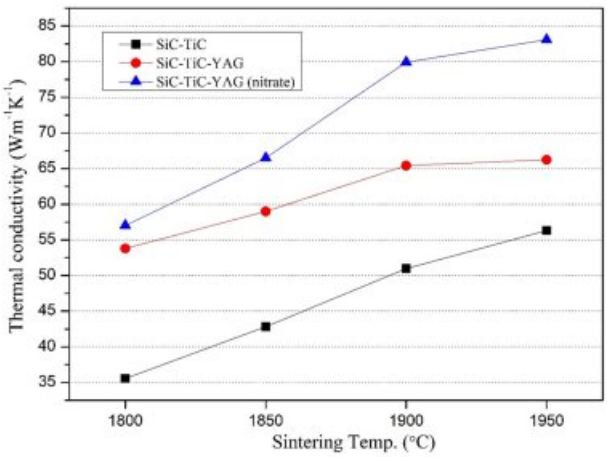

Fig. 9. Variation of thermal conductivity of SiC-TiC composites with the sintering temperature.

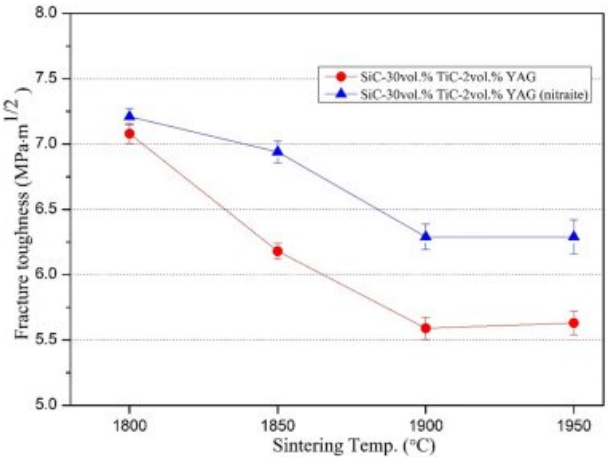

Fig. 7. Variation of fracture toughness of SiC-TiC composites with the sintering temperature.

expansion coefficients and elastic modulus differences between the matrix and dispersed ceramic particles. The fracture toughness is enhanced by the residual stress on the matrix when the coefficient of thermal expansion of the added particles is greater than that of the matrix. Therefore, in the SiC-TiC composites, the thermal expansion coefficients of SiC and TiC are 4.5×10^{-6} K^{-1} and 7.4×10^{-6} K^{-1}, respectively, so that compressive residual stress is formed on the SiC because of the smaller coefficient, and the toughness is enhanced compared to monolithic SiC [30, 31].

To understand the fracture mode and the strengthening mechanism of the SiC-TiC composite in more detail, the cracks induced by Vickers indenters were observed by FE-SEM and shown in Fig. 8. It was confirmed that crack toughening and branching occurred in all compositions containing nitrate and oxide sintering aids, which prevented crack propagation and enhanced fracture toughness [32].

Fig. 9 is the thermal conductivity measurement result of the SiC-TiC composite. As the sintering temperature increased and densification proceeded, the thermal conductivity increased. However, the composite without sintering aid showed low thermal conductivity due to low density and low porosity inside the specimen.

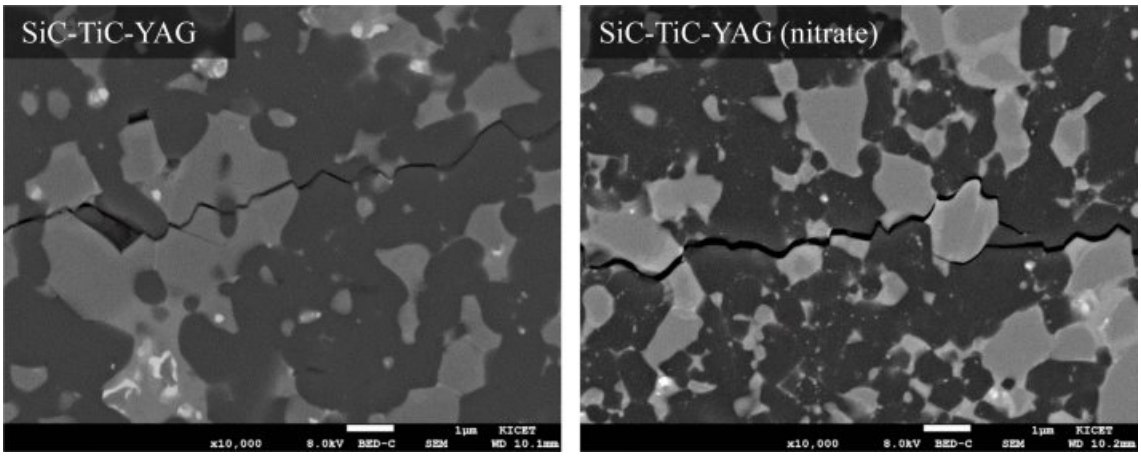

Fig. 8. SEM image of the crack paths of SiC-TiC composites sintered at 1,900 °C.

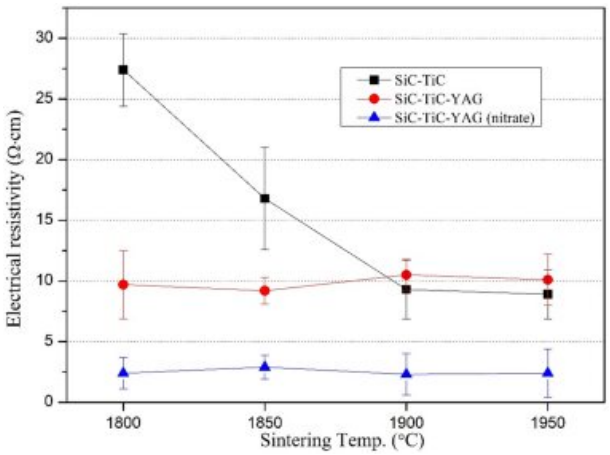

Fig. 10. Variation of electrical resistivity of SiC-TiC composites with the sintering temperature.

STYN sample showed the best thermal conductivity as 83 W/mK at sintering temperature of 1,950 ºC. Fig. 10 shows the electrical resistance of the SiC-TiC composite according to the sintering temperature. In the composition without the sintering aid, the electrical resistance decreased significantly as the densification progressed. When sintering was performed at 1,900 and 1,950 ºC, the value was lower than that of the STY composition containing the oxide sintering aid. This may be because YAG, which has high electrical resistance, is present at the grain boundaries and triple points of SiC and TiC, thereby lowering the overall electrical conductivity. On the other hand, in the composition containing nitrate sintering aid, the YAG phase was found to have the lowest electrical resistance, because it exists finely and uniformly compared to the oxide composition, and it was found to have a low electrical resistance of 2.3 Ω·cm at 1,900 ºC.

Conclusion

In this study, compact and uniform SiC-30 vol% TiC composites having a relative density of about 99.9% at 1,900 ºC could be prepared by hot press sintering method adding aluminum nitrate and yttrium nitrate as sintering aids. Nitrate sintering aid is dissolved in ethanol and can be uniformly mixed with the raw material, which promotes densification of SiC-TiC composite at a lower temperature than oxide sintering aid, and forms a uniform and fine YAG phase to improve mechanical properties of the sintered body. With sintering at 1,900 ºC, the bending strength was 652.3 MPa, the Vickers hardness was 25.14 GPa, and the fracture toughness was 6.29 MPa·$m^{1/2}$. Since the electrical conductivity of SiC-TiC ceramic composites is greatly influenced by the grain size of the components constituting the matrix and the amounts of additives and uniform dispersion, SiC-TiC composites with the electrical resistance of 2.3Ω·cm could be prepared at 1,900 ºC sintering temperature with the addition of nitrate.

Acknowledgment

This work was supported by the Technology Innovation Program (10067558, Development of functional watches with ceramic composite) funded by the Ministry of Trade, Industry & Energy (MOTIE, Korea)

References

1. Y.G. Gogotsi, P. Kofstad, M. Yoshimura, and K.G. Nickel, Diam. Relat. Mater. 5[2] (1996) 151-162.
2. A. Noviyanto and D. Yoon, Curr. Appl. Phys. 13[1] (2013) 287-292.
3. O. Lopes, A. Ortiz, F. Guibertuau, and N. Padture, J. Eur. Ceram. Soc. 27[11] (2007) 3351-3357.
4. S. Prochazka and R. M. Scanlan, J. Am. Ceram. Soc. 58[12] (1975) 72-72.
5. R.A. Alliegro, L.B. Coffin, and J.R. Tinklepsugh, J. Am. Ceram. Soc. 39[11] (1956) 386-389.
6. D. Sciti and A. Bellosi, J. Mater. Sci. 35[15] (2000) 3849-3855.
7. K. Biswas, G. Rixecker, and F. Aldinger, J. Eur. Ceram. Soc. 23[7] (2003) 1099-1104.
8. M. Balog, P. Šajgalík, M. Hnatko, Z. Lenčéš, F. Monteverde, J. Kečkéš, and J.-L. Huang, J. Eur. Ceram. Soc. 25[4] (2005) 529-534.
9. S. Kaur, R. Riedel, and E. Ionescu, J. Eur. Ceram. Soc. 34[15] (2014) 3571-3578.
10. H. Harima, Microelectron. Eng. 83[1] (2006) 126-129.
11. K.J. Kim, S.H. Jang, Y.W. Kim, B.K. Jang, and T. Nishimura, Ceram. Int. 42[15] (2016) 17892-17896.
12. J.R. Jenny, D.P. Malta, St G. Müller, A.R. Powell, V.F. Tsvetkov, H. McD Hobgood, R. C. Glass, and C. H. Carter Jr., J. Electron. Mater. 32[5] (2003) 432-436.
13. F. Siegelin, H.J. Kleebe, and L.S. Sigl, J. Mater. Res. 18[11] (2003) 2608-2617.
14. K.J. Kim, J.H. Eom, Y.W. Kim, W.S. Seo, M.J. Lee, and S.S. Hwang, Ceram. Int. 43[15] (2017) 5343-5346.
15. G. Augustine, V. Balakrishna, and C.D. Brandt, J. Cryst. Growth 211[1-4] (2000) 339-342.
16. T.Y. Cho, Y.W. Kim, and K.J. Kim, J. Eur. Ceram. Soc. 36[11] (2016) 2659-2665.
17. J. Cabrero, F. Audubert, and R. Pailler, J. Eur. Ceram. Soc. 31[3] (2011) 313-320.
18. M. Khodaei, O. Yaghobizadeh, N. Ehsani, H.R. Baharvandi, and A. Dashti, Ceram. Int. 44[14] (2018) 16535-16542.
19. O. Agac, M. Gozutok, H.T. Sasmazel, A. Ozturk, and J. Park, Ceram. Int. 43 (2017) 10434-10441.
20. H. Endo, M. Ueki, and H. Kubo, J. Mater. Sci. 26 (1991) 3769-3774.
21. D. Ahmoye, D. Bucevac, and V.D. Krstic, Ceram. Int. 44[12] (2018) 14401-14407.
22. D. Shaoming, J. Dongliang, T. Shouhong and G. Jingkun, J. Mater. Sci. Lett. 15 (1996) 394-396.
23. H.G. An, Y.W. Kim and J.G. Lee, J. Eur. Ceram. Soc. 21[1] (2001) 93-98.
24. G.C. Wei and P.F. Becher, J. Am. Ceram. Soc. 67[8] (1984) 571-574.
25. M. Khodaei, O. Yaghobizadeh, N. Ehsani, and H.R. Baharvandi, Int. J. Refract. Met. Hard Mater. 76 (2018)

141-148.
26. J.Y. Kim, T. Iseki, and T. Yano, J. Am. Ceram. Soc. 79[10] (1996) 2744-2746.
27. T. Miyoshi. N. Sagawa, and T. Sasa, J. Jpn. SpC. Mech. Eng. A 51[471] (1985) 2489-2497.
28. Z. Zhang, X. Du, W. Wang, Z. Fu, and H. Wang, Int. J. Refract. Met. Hard Mater. 41 (2013) 270-275.
29. Y. Azizian-Kalandaragh, A. Sabahi Namini, Z. Ahmadi, and M. Shahedi Asl, Ceram. Int. 44[16] (2018) 19932-19938.
30. M. Taya, S. Hayashi, A.S. Kobayashi, and H.S. Yoon, J. Am. Ceram. Soc. 73[5] (1990) 1382-1391.
31. S.M. So, W.H. Choi, K.H. Kim, J.S. Park, M.S. Kim, J. Park, Y.S. Lim, and H.S. Kim, Ceram. Int. 46[7] (2020) 9575-9581.
32. M.S. Asl, Z. Ahmadi, A.S. Namini, A. Babapoor, and A. Motallebzadeh, Ceram. Int. 45[16] (2019) 19808-19821.